A Novel Architecture of a Heptadentate Macroacyclic 2,6-Bis [(3-methoxy salicylidene) Hydrazino Carbonyl] Pyridine Towards Lanthanides: A Synthetic and Structural Studies of Dinuclear Lanthanide (III) Complexes

KALAGOUDA B. GUDASI*, RASHMI V. SHENOY, RAMESH S. VADAVI, MANJULA S. PATIL and SIDDAPPA. A. PATIL
Department of Chemistry, Karnatak University, 580 003, Dharwad, Karnataka, India

Abstract

Reaction of $Ln(NO_3)_3$ with 2,6-bis[(3-methoxysalicylidene)hydrazino carbonyl]pyridine (BMSPD) afforded binuclear complexes of the type $[Ln_2(BMSPD)(NO_3)_2(H_2O)_5] \cdot 3H_2O$ in case of La(III), Pr(III), Nd(III), Sm(III), Eu(III), Gd(III), Tb(III) and Dy(III), and $[Ln_2(BMSPD)(NO_3)_2(H_2O)_5]$ in case of Y(III). The mode of coordination of ligand and the conformational changes on complexation with lanthanides was studied based on elemental analysis, magnetic studies, TG/DTA, IR, ^{1}H-NMR, Electronic, EPR and Fluorescence spectral studies. The ligand coordinates to one metal centre through enolized deprotonated carbonyls and pyridine nitrogen whereas doubly deprotonated phenolate oxygens and two hydrazonic nitrogens ligate to another lanthanide centre. Both the metal ions are in eight-coordination environments. The ligand and complexes were further tested for antifungal and antibacterial activities.

Introduction

In nature, certain catalytic processes have been brought about by enzymes possessing two or three metal centers in their active sites. Hence in biomimetic catalysis, synthesis of molecules mimicking the activity analogous to enzymes has received a lot of attention [1–4]. Especially trivalent metal ions are known to exhibit high catalytic activity due to their high Lewis acidity. Further, the presence of two metal ions gives rise to many possible modes of Lewis acid catalysis [5, 6]. For example, dinuclear Praseodymium (III) and Europium (III) complexes accelerate cleavage of supercoiled DNA twice as fast as compared to metal ions alone [7]. Apart from these, homo- and hetero-polynuclear lanthanide complexes possess unique physico-chemical properties [8, 9] and exhibit potential applications in biomedical diagnostics [10], fluorescence imaging [11], MR imaging [12], tunable photonic devices [13], metalloorganic chemical vapor deposition [14] and sol–gel technology [15].

It is also known that polyfunctional hydrazones possessing amide and azomethine functions yield homo- or hetero-dinuclear complexes of interest in areas such as multimetallic enzymes and homo- or hetero-geneous

catalysis [16], thus providing a context for design and synthesis of new structural types. This, and the propensity of lanthanides to prefer higher coordination numbers by forming dinuclear species may lead to compounds exhibiting significant architectural novelty and potential functionality as catalysts as a consequence of incorporation of lanthanides in its structure.

Keeping the above in mind, we have designed and synthesized a potential heptadentate ligand, 2,6-bis[(3-methoxysalicylidene)hydrazinocarbonyl]pyridine (BMSPD) having multiple coordinating sites that can bind and stabilize the complex, and flexible groups that accommodate two or more metal atoms; a step towards achieving our goal.

The ligand BMSPD can behave in two ways, as reported earlier [17, 18]; (a) as a compartmental ligand (Figure 1) in case of inner-transition metal, coordinating in two different modes, as tridentate in the terminal compartment coordinating through hydrazonic carbonyl, hydrazonic nitrogen and phenolic oxygens and as tridentate in the central chamber coordinating through pyridyl nitrogen and two hydrazonic oxygens or (b) as a macroacyclic ligand (Figure 2) incorporating two metals, with the outer metal atom causing cleft closure through two phenolic oxygens leading to a macroacyclic complex, or (c) as shown in Figure 3.

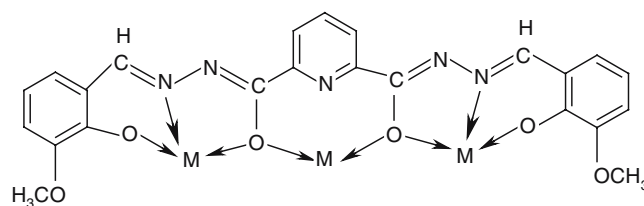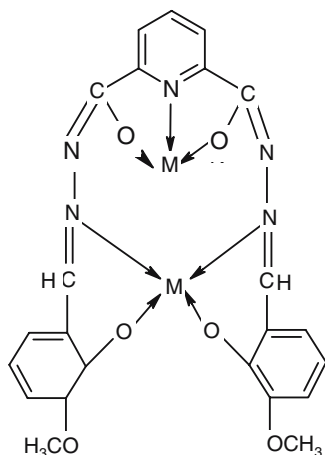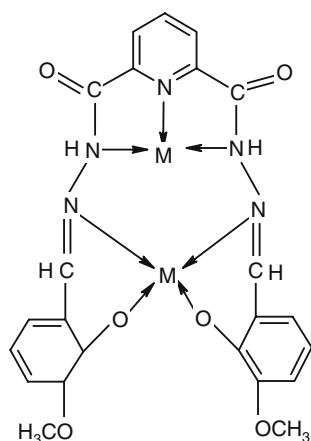* Author for correspondence. E-mail: kbgudasi@rediffmail.com

Figure 1.

Figure 2.

Figure 3.

Experimental

Physical measurements

Elemental analysis were performed on a Carlo Erba Strumentazione (Italy) CHN analyzer. Mass spectrum of ligand was recorded on a Thermofinnigan 1020 automated GC MS. Molar conductivities were obtained in DMSO (10^{-3} M) using an ELICO-CM 82 conductivity bridge having a dip type conductivity cell having platinum electrodes. Magnetic moments were obtained on a Faraday balance using Hg[Co(NCS)$_4$] as calibrant and diamagnetic corrections were made using Pascal's constants [19]. The IR spectra were obtained from KBr pellets with a Nicolet 170 SX FT-IR spectrophotometer in the range 400–4000 cm^{-1}. ^{1}H-NMR spectra were

recorded on a JEOL-AMX-400 NMR spectrophotometer in D$_6$-DMSO using TMS as an internal reference. Electronic spectra were recorded in DMSO solution, with a Hitachi 2001 spectrophotometer. Fluorescence spectra were measured on a F-2000 Hitachi fluorescence spectrophotometer. EPR spectra of the Gd(III) complex were obtained on a Varian E-4X band spectrophotometer. TG/DTA thermograms were recorded on a Perkin–Elmer (Pyris Diamond) Analyzer in nitrogen atmosphere at a heating rate of 10 °C/min and a maximum temperature of 1000 °C. The metal contents were determined by complexometric titrations with EDTA using xylenol orange as an indicator [20].

Preparative methods

All chemicals used were of AR grade and used without further purification. The lanthanide (III) nitrates were obtained by heating lanthanide oxides (99.9%, Indian Rare Earths Ltd.) with aqueous nitric acid (1:1) and subsequent evaporation. Dipicolinic acid (Spectrochem) and o-Vanillin (Fluka) were used.

The preparation of the ligand follows the reaction sequence reported in Scheme 1.

### Preparation of Dipicolinic acid hydrazide

Pyridine-2,6-dicarboxylic acid (1.67 g, 0.01 mol) and thionyl chloride (25 cm^3) were refluxed in anhydrous condition for 4–5 h till a clear solution was obtained. The excess thionyl chloride was then removed under reduced pressure. After cooling in ice, dry ethanol (30 cm^3) was added and further refluxed for 5–6 h to obtain the diethyl ester of dipicolinic acid. This was further treated with hydrazine hydrate (0.96 ml, 0.02 mol) and refluxed for 3 h. On cooling, a thick precipitate was obtained which was further recrystallized from hot water to give long colorless needles of dipicolinic acid hydrazide.

Yield: 82%; M.p.: 285 °C.

The ligand BMSPD was prepared by slight modification of literature method [18].

Synthesis of 2,6-Bis[(3-methoxysalicylidene)hydrazino carbonyl] pyridine

Dipicolinic acid hydrazide (1.95 g, 0.01 mol) and o-Vanillin (3.04 g, 0.02 mol) were refluxed in 60 cm^3 of methanol for 4 h. The thick yellow precipitate obtained was filtered, washed with alcohol and air-dried. It was
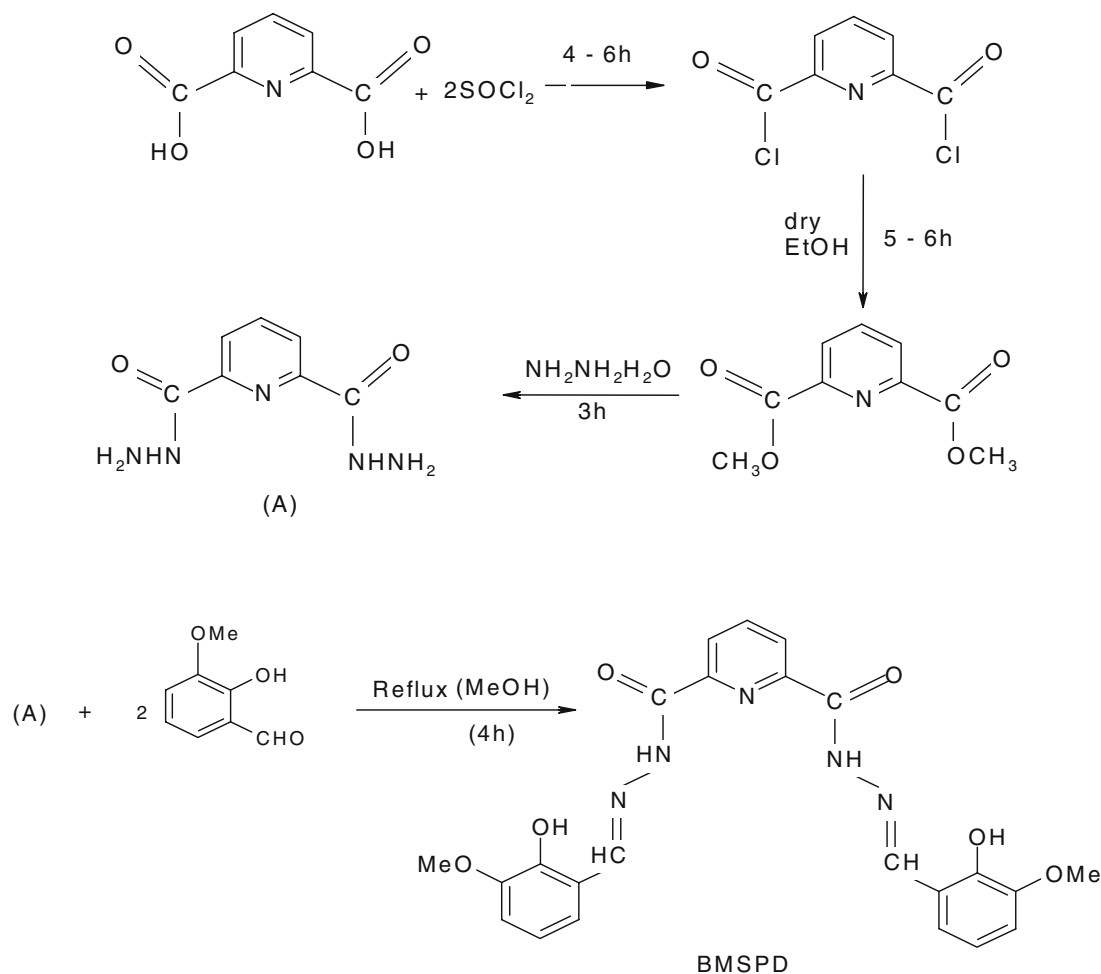
Scheme 1.

further recrystallised from 2-ethoxy ethanol to yield yellow crystals of BMSPD.

Yield: 90%; M.p. = 270–272 °C

Synthesis of complexes

A solution of Ln(NO$_3$)$_3$ (0.002 mol) and BMSPD (0.463 g, 0.001 mol) was refluxed in EtOH (25 cm^3) for 1 h. The pH of the solution was then raised to 6.5 by adding sodium acetate (dissolved in minimum amount of alcohol) and further refluxed for 6 h. The resulting solution was concentrated to one third of the original volume, which lead to the formation of a microcrystalline powder that was isolated and dried under vacuum. In some cases, a small amount of diethyl ether was slowly infused to aid precipitation.

Yield: 78%; M. p.: > 250°

Results and Discussion

Microanalytical and molar conductivity data

The microanalytical, magnetic and molar conductivity data for the complexes characterized are presented in Table 1. The reaction of Ln(NO$_3$)$_3$ with 2,6-bis

[(3-methoxysalicylidene)hydrazinocarbonyl] pyridine (BMSPD) results in the formation of binuclear complexes with the general formula [Ln$_2$(BMSPD)(NO$_3$)$_2$ (H$_2$O)$_5$]·3H$_2$O in case of La(III), Pr(III), Nd(III), Sm(III), Eu(III), Gd(III), Tb(III) and Dy(III), and [Ln$_2$(BMSPD)(NO$_3$)$_2$(H$_2$O)$_5$] in case of Y(III) (Table 1). The complexes are stable, non-hygroscopic and orange yellow in color. They are sparingly soluble in ethanol, methanol, DMF and DMSO and are insoluble in chloroform, benzene, acetone and ethyl acetate.

The molar conductance values of the complexes in DMSO at 10^{-3} M lie in the range 0.58–0.71 Ω^{-1} cm^2 mol^{-1} indicating their non-electrolytic nature [21].

IR spectra

The IR spectral data of the ligand and complexes is given in Table 2. In the free ligand, the broad weak bands in the region 2839–3246 cm^{-1} is indicative of intramolecular hydrogen bonding (vOH–N=C) [22]. The bands at 3246 and 3456 cm^{-1} are assigned to v(OH) and v(NH) respectively [22]. The disappearance of these bands on complexation indicate breakdown of hydrogen bonding due to bond formation between metal and phenolic oxygen via deprotonation [18]. This leads to closure of the cleft between the two phenolic groups in

Table 1. Analytical, magnetic moment and conductance data of BMSPD and its Ln(III) complexes

Compound	Found (Calcd.) (%)				Magnetic moment[a]	Molar conductivity[b]
	M	C	H	N		
BMSPD	–	57.32 (57.38)	4.71 (4.78)	14.50 (14.55)	–	–
C1 [La$_2$(BMSPD)(NO$_3$)$_2$(H$_2$O)$_5$]·3H$_2$O	27.66 (27.53)	27.47 (27.51)	3.27 (3.17)	9.84 (9.70)	Dia	0.62
C2 [Pr$_2$(BMSPD)(NO$_3$)$_2$(H$_2$O)$_5$]·3H$_2$O	27.72 (27.82)	27.31 (27.25)	3.19 (3.25)	9.59 (9.67)	3.61	0.59
C3 [Nd$_2$(BMSPD)(NO$_3$)$_2$(H$_2$O)$_5$]·3H$_2$O	28.19 (28.29)	27.15 (27.07)	3.31 (3.23)	9.58 (9.61)	3.65	0.66
C4 [Sm$_2$(BMSPD)(NO$_3$)$_2$(H$_2$O)$_5$]·3H$_2$O	28.94 (29.11)	26.84 (26.75)	3.22 (3.19)	9.50 (9.49)	1.75	0.70
C5 [Eu$_2$(BMSPD)(NO$_3$)$_2$(H$_2$O)$_5$]·3H$_2$O	29.36 (29.39)	26.73 (26.66)	3.21 (3.18)	9.51 (9.46)	3.34	0.74
C6 [Gd$_2$(BMSPD)(NO$_3$)$_2$(H$_2$O)$_5$]·3H$_2$O	30.17 (30.08)	26.44 (26.39)	3.12 (3.15)	9.42 (9.37)	7.83	0.65
C7 [Tb$_2$(BMSPD)(NO$_3$)$_2$(H$_2$O)$_5$]·3H$_2$O	30.42 (30.30)	26.19 (26.31)	3.24 (3.14)	9.37 (9.34)	9.57	0.67
C8 [Dy$_2$(BMSPD)(NO$_3$)$_2$(H$_2$O)$_5$]·3H$_2$O	30.93 (30.89)	26.21 (26.13)	3.15 (3.12)	9.31 (9.28)	10.47	0.71
C9 [Y$_2$(BMSPD)(NO$_3$)$_2$(H$_2$O)$_5$]	20.71 (20.80)	33.58 (33.69)	3.59 (3.62)	11.51 (11.46)	Dia	0.58

[a]B.M; [b]Ohm^{-1} cm^2 mol^{-1}; Dia = diamagnetic.

Table 2. Diagnostic IR bands (cm^{-1}) of BMSPD and its Ln(III) complexes

Compound	v(OH)	v(NH)	v(C=O)	v(C=N)	Py 'N'	–NO$_3$ bands					
						v_4	v_1	v_6	v_2	v_3	v_5
BMSPD	3246b	3456s	1677s	1609s*	1586s	–	–	–	–	–	–
C1	3388b	–	–	1610s	1560s	1550s	1301m	840m	1017m	739m	671w
C2	3413b	–	–	1607s	1559s	1554s	1301m	843m	1017m	739m	675w
C3	3406b	–	–	1610s	1560s	1554s	1301m	839m	1014m	738m	672w
C4	3419b	–	–	1610s	1567s	1555s	1301m	841m	1015m	739m	675w
C5	3431b	–	–	1610s	1560s	1550s	1303m	840m	1019m	739m	671w
C6	3419b	–	–	1610s	1560s	1555s	1303m	842m	1017m	738m	674w
C7	3413b	–	–	1610s	1567s	1555s	1304m	843m	1017m	745m	673w
C8	3413b	–	–	1604s	1567s	1555s	1302m	843m	1017m	741m	684w
C9	3413b	–	–	1616s	1567s	1550s	1304m	842m	1018m	737m	685w

s, strong; b, broad; m, medium; w, weak.
* Observed for –CH=N of ligand.

the ligand molecule. The pyridine ring stretching vibrations appear at 1590, 1578, 1461 and 1446 cm^{-1}. The bands at 999 and 775 cm^{-1} are assigned to the pyridine-CH-in-plane bend and pyridine CH-out-of-plane bend respectively [23].

The amide bands are observed at 1677 (vC=O, NH I), 1536 (vCN + δNH, NH II), 1248 (vNH, NH III), 653 (ΦC=O, NH IV) and 470 cm^{-1} (πC=O, NH VI), respectively [24]. On complexation, the vC=O, amide I band disappears, and a new band appears at 1610 cm^{-1} which is characteristic of v>C=N–N=C< group [17, 25, 26]. This is indicative of the ligation of carbonyl group via enolization and deprotonation, and the coordination of vC=N to the metal, which is further supported by the disappearance of the vNH stretching

band at 3456 cm^{-1} and the amide bands [26, 27]. In the complexes, the pyridine ring stretching vibrations at 1590 and 1578 cm^{-1} merge and shift towards lower frequency giving a broad band at 1560 cm^{-1} whereas the bands at 1461 and 1446 cm^{-1} also merge to give a band at 1455 cm^{-1}. The pyridine CH-in-plane bend and pyridine CH-out-of-plane bend vibrations are shifted to higher frequencies, 1017 and 782 cm^{-1} respectively. These changes indicate the involvement of pyridine nitrogen in coordination [28]. In all the complexes except Y(III) complex, the broad diffuse bands of medium intensity in the region 3600–3500 cm^{-1} are assigned to –OH stretching modes of lattice water. A band between 850 and 900 cm^{-1} is assigned to the rocking frequency of the coordinated water molecules [29], which is further

supported by the TG studies. The absorptions due to nitrate ions provide information about their mode of coordination. The presence of strong absorptions bands at 1550–1555 (v_4), 1301–1304 (v_1) and 738–745 cm^{-1} (v_3) indicates the presence of coordinated nitrate groups. The two highest frequency bands are separated by *ca.* 249 cm^{-1}. The magnitude of this separation is typical of bidentate coordination of nitrates [30, 31].

NMR spectra

The ^{1}H-NMR spectra of BMSPD and its La(III) complex were obtained in D$_6$-DMSO. The proton assignments (Figure 4, Table 3) have been made based on literature data [32, 33] and comparisons with proton assignments of dipicolinic acid [34] and *o*-vanillin [35].

In the "free" ligand, the signals due to aromatic protons are observed in the region 6.89–8.38 ppm. A single set of signals are obtained, indicating the two arms of the ligand are magnetically equivalent on the NMR time scale. Two singlets at 12.41 and 10.66 ppm are due to two protons each of –OH and –NH respectively (D$_2$O exchangeable) [17]. A sharp singlet in the upfield region at 3.85 ppm is due to the –OCH$_3$ group and accounts for six protons [32].

A multiplet at 8.30 ppm is assigned to H4 (Figure 4) of pyridine ring whereas a doublet at 8.38 ppm corresponds to H3 and H5 of the dipicolinic moiety. A triplet at 6.91 ppm corresponds to H10 and H10′. A doublet at 7.08 ppm is ascribed to H11 and H11′ whereas another doublet at 7.30 ppm is due to H9 and H9′. A singlet at 8.97 ppm is ascribed to protons of the two –CH=N groups.

The ^{1}H-NMR spectrum of the La(III) complex shows the absence of –NH signal confirming the coordination of carbonyl oxygen to metal via enolization and deprotonation. The absence of the –OH proton (12.41 ppm) in the spectrum of the complex suggests metallation through the phenolato oxygens.

Table 3. ^{1}H-NMR spectral data (ppm) of BMSPD and its La(III) complex

Proton	PPDA	La(III) Complex
–OH	12.41 (s, 2H) (exchanges with D$_2$O)	–
–NH	10.66 (s, 2H) (exchanges with D$_2$O)	–
–CH	8.97 (s, 2H)	8.98, 9.07(s)
H3 & H5	8.38(d, $J = 7.2$ Hz)	8.47 (m, 3H)[a]
H4	8.30(m)	
H9 & H9′	7.30 (d, $J = 7.6$ Hz)	7.04, 7.18 (d, $J = 7.5$ Hz)
H10 & H10′	6.91 (t, $J = 7.9$ Hz)	6.81 (m, 4H)[b]
H11 & H11′	7.08 (d, $J = 7.8$ Hz)	
–OCH$_3$	3.85 (s, 6H)	3.82 (s, 6H)

s, singlet; d, doublet; t, triplet; m, multiplet
[a]Due to poor solubility in DMSO-d$_6$, the splitting pattern was not clearly observed.
[b]the signals consisting of a double and a multiplet merge to give a multiplet.

The coordination of phenolic oxygen through deprotonation is also confirmed by the upfield shift of H9/9′, H10/10′ and H11/11′, which thereby shield the phenyl protons [17].

A double set of signals was obtained for the complex indicating non-equivalence of all aromatic rings. The molecule thus possesses nine non-equivalent aromatic protons. Since the electronic environments of the aromatic hydrogen atoms are very similar, their signals appear in a narrow chemical shift range.

The H3, H5 and H4 signals consisting of a doublet and a multiplet merge to give a multiplet, which is shifted downfield (8.47 ppm) indicating the coordination of pyridine nitrogen to the metal [36].

Magnetic and EPR spectral studies

All the complexes except La(III) and Y(III) are paramagnetic in nature (Table 1). The magnetic moments of the complexes do not deviate much from Van Vleck [37]
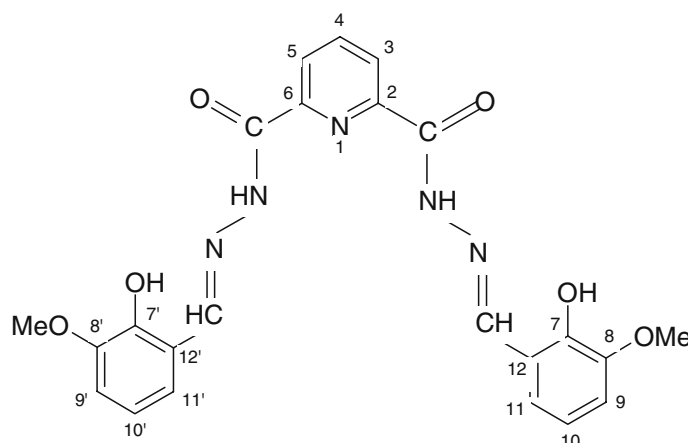

Figure 4. Proton assignation for the NMR spectra of BMSPD .

and Hund's values [38] indicating little participation of 4f electrons in bonding. However Eu(III) and Sm(III) show anomalous magnetic moments. This is due to low J–J separation, which leads to thermal population of higher energy levels and shows susceptibility due to first order Zeeman Effect [39, 40].

Non-deviation of magnetic moment values indicates absence of metal–metal interaction between the adjacent metal atoms either through bridging or super-exchange mechanism.

Gd(III) has an $^8S_{7/2}$ single ion ground state and a spin value (I) of 3/2. The energy level of lowest excited state is very high with no contribution from orbital angular momentum and the anisotropic effect.

The EPR spectra of the Gd(III) complex showed a broad resonance peak (at both RT and LNT) with $\langle g \rangle$ = 2.20 (at RT) and $\langle g \rangle$ = 2.21 (at LNT) compared to free-ion value $\langle g \rangle$ of TCNE (2.00277). It was observed that zero-field hyperfine splitting was absent; instead a broad band was obtained. Inhomogeneous broadenings are due to unresolved hyperfine couplings and distributions in Hamiltonian parameters, which are called strains. It is likely that presence of water molecules leads to formation of random H-bonds between these molecules and the complex leading to distortions in the coordination sphere. These distortions further give rise to strain (g strain for the g tensor distribution, D-strain for the zero-field splitting distribution) which lead to broad asymmetric EPR lines [41–43].

Further, similar g values and line widths (at both RT and LNT) indicate line widths are independent of temperature [44].

Electronic spectra

The electronic spectrum of the ligand is characterized by three bands at 314, 308 and 304 nm, the former two bands are due to π–π* and the latter due to n–π* transitions. The spectra of the complexes is similar to that of ligand except for a slight shift either to higher or lower energy levels. No absorption bands due to f–f transitions could be observed in the visible region of the spectrum. This may be attributed to intense charge-transfer transitions that obscure the f–f bands. However Pr(III) and Nd(III) showed few low intensity bands in the visible

region. The shape and position of the hypersensitive transitions are similar to that of eight-coordinated complexes, as reported by Karraker [45]. The transitions of the representative Nd(III) and Pr(III) complexes are given in Table 4.

Compared to the free aquo ion, these bands have been shifted to lower energy levels. Jorgensen [46] attributes this shift in bands to the effect of crystal fields upon the interelectronic repulsion among the 4f electrons i.e. to lowering of the interelectronic repulsion parameter (β) in the complexes. Table 5

The various spectral parameters like bonding parameter ($b^{1/2}$), Sinha's covalency parameter (δ), nephelauxetic parameter (β) and angular covalency parameter (η) [47–49] have been calculated.

The Sinha's parameter [δ] is taken as a measure of covalency and is given by,

$$\delta = (1 - \beta_{av})/\beta_{av} \times 100$$

where β_{av} is the average value of the ratio of $v_{complex}/v_{aquo}$.

The bonding parameter ($b^{1/2}$), the magnitude of which suggests the comparative involvement of the 4f orbitals in metal–ligand bonding, is related to the nephelauxetic ratio β and is given by the expression,

$$b^{1/2} = [(1 - \beta_{av})/2]^{1/2}.$$

β values being less than unity and positive values of $b^{1/2}$ and δ indicate slight metal–ligand covalent bonding.

Fluorescence spectral studies

The fluorescence spectra of BMSPD and its Ln(III) complexes were recorded in DMSO at room temperature. Only Sm(III), Eu(III), Dy(III) and Tb(III) complexes show corresponding metal luminescence whereas the remaining complexes showed the luminescence of the ligand at excitation of 380 nm.

The emission spectrum of Eu(III) complex is dominated by ligand absorptions onto which weak Eu(III) absorptions are superimposed. The emission spectrum is typical of Eu(III) and shows an emission line due to $^5D_0 \rightarrow {}^7F_0$ transition consisting of the component at 586 nm. The $^5D_0 \rightarrow {}^7F_1$ transition shows a component at 590 nm whereas the $^5D_0 \rightarrow {}^7F_2$ transitions appear at

Table 4. Electronic spectral data (in cm^{-1}) and related bonding parameters of a few Ln(III) complexes of BMSPD

Complex	Assignments	λ_{max} of Ln^{+3} ion	λ_{max} of complex	β	Related parameters
[Pr$_2$(BMSPD)(NO$_3$)$_2$(H$_2$O)$_5$]·3H$_2$O	$^3H_4 \rightarrow {}^1D_2$	16950	16880	0.99587	δ = 0.64108
	$\rightarrow {}^3P_0$	20830	20624	0.990110	$b^{1/2}$ = 0.05643
	$\rightarrow {}^3P_1$	21282	21158	0.99417	η = 0.080067
	$\rightarrow {}^3P_2$	22466	22340	0.99439	
				β_{av} = 0.99363	
[Nd$_2$(BMSPD)(NO$_3$)$_2$(H$_2$O)$_5$]·3H$_2$O	$^4I_{9/2} \rightarrow {}^4F_{3/2}$	11515	11420	0.99174	δ = 0.083287
	$\rightarrow {}^2H_{9/2}$	12475	12456	0.99847	$b^{1/2}$ = 0.06426
	$\rightarrow {}^4F_{7/2}$	13550	13347	0.98501	η = 0.091262
				β_{av} = 0.99174	

Table 5. Antibacterial and Antifungal activity data of BMSPD and its Ln(III) complexes

Compound	Antifungal		Antibacterial	
	PN	AN	PA	BC
BMSPD	–	+	+	–
C1	+	+	+	+ +
C2	+	+	+	+ +
C3	+	+	+	+ +
C4	+	+	+	+ +
C5	+	+	+	+ +
C6	+	+	+	+ +
C7	+	+	+	+ +
C8	+	+	+	+ +
C9	+	+	+	+ +
Grisofulvin	+ + +	+ + +	–	–
Norfloxacin	–	–	+ + +	+ + +

Key to interpretation: (−) No zone = inactive; 1–5 mm (+) = Less active; 6–10 mm (+ +) = moderately active; 11–15 mm (+ + +) = highly active; 16–20 mm (+ + + +) = super active

609 and 616 nm. It is observed that relative intensities of $^5D_0 \rightarrow {}^7F_1$ and $^7F_2$ emissions are sensitive to ligand environment thus reflecting the hypersensitive character of the $^5D_0 \rightarrow {}^7F_2$ transition. This situation can be assigned to an eight-coordinate structure (D$_2$d symmetry) [50] corresponding to a dodecahedral geometry [51]. In case of Sm(III) complex, the emission spectrum shows a weak component at 558 nm and a broad one at 556 nm due to $^4G_{5/2} \rightarrow {}^6H_{5/2}$ transition.

The effect of temperature (ranging from 15, 25, 35 and 45 °C) and concentration (10^{-3} M and 10^{-4} M) on the fluorescence intensity was also studied. Increase in fluorescence intensity was observed at low temperature (15 °C) and high temperature (45 °C) whereas at other temperatures there was a decrease in intensity. Similarly at higher concentration (10^{-3} M) there was a decrease in intensity compared to that at lower concentration (10^{-4} M), which can be attributed to the self-quenching effect [52]. However, the low overall intensities of the complexes may probably be due to presence of coordinated water molecules, which act as fluorescent quenchers or, due to quenching of the excited lanthanide ion by vibrational energy transfer [53]. Deactivation of excited lanthanide ion may occur in solution due to vibrational energy transfer to high-energy vibration of OH of the bound ligand or solvent. Since phenolic OH of the ligand is deprotonated on complexation, we could suppose that quenching occurs via multiphonon-like processes due to the –OH stretching vibrations of the coordinated water molecules. Hence removal of these quenching –OH oscillators may lead to an increase of the metal based emission [54].

Thermal analysis

Thermal analyses on two representative complexes have been carried out in the range 25–1000 °C in-order to ascertain the thermal behavior of ligand and nature of

water molecules. In case of [La$_2$(BMSPD)(NO$_3$)$_2$(H$_2$O)$_5$]·3H$_2$O, the complex undergoes a three step decomposition process with the first weight loss of 5.40% between 50 and 110 °C corresponding to the loss of three lattice held water molecules (Calc: 5.36%). The second weight loss in the range 110–177 °C is due to loss of five coordinated water molecules (Obs: 8.89%; Calc: 8.93%) and is indicated by a strong endothermic peak on DTA curve. The next weight loss of 62.69% (Calc: 62.58%) between 450–650 °C agrees with the loss of two coordinated nitrate molecules and one ligand molecule. Finally, the most stable oxide La$_2$O$_3$ is formed. The observed metal percentage (27.37%) is in good agreement with calculated value (27.53%).

In case of [Y$_2$(BMSPD)(NO$_3$)$_2$(H$_2$O)$_5$], the mass loss (Obs: 17.66%; Calc: 17.28%) in the temperature range 120–290 °C accounts for five coordinated water and one coordinated nitrate molecule. A strong endothermic peak is observed on DTA curve at 290 °C. The second and third step of decomposition in the temperature range 300–500 °C involves loss of another coordinated nitrate and a ligand molecule (Obs: 61.53%; Calc: 61.41%). The metal percentage (20.65%) calculated from the stable Y$_2$O$_3$ formed was in good agreement with the calculated value (20.80%). These values support the elemental analysis for 2:1 (M:L) stoichiometry.

Biological activity

The antibacterial and antifungal activities of BMSPD and its lanthanide (III) complexes were evaluated against the bacteria *Pseudomonas aeuregenosa* (PA) (Gram –ve) and *Bacillus cirroflagellosus* (BC) (Gram + ve) and the fungi *Aspergillus niger* (AN) and *Penicillium notatum* (PN), by the cup-plate method [55]. The concentration of the compound used for testing was 1 mg/ml in DMSO. Grisofulvin and Norfloxacin were the standards used against fungi and bacteria respectively.

The results of the inhibitory activity indicate the ligand is less active against AN and PA. The complexes are less active against PN, AN and PA. However, in case of BC the complexes exhibited moderate activity compared to the standards.

Conclusion

Based on the analytical and spectral studies, the present lanthanide complexes have been formulated as [Ln$_2$(BMSPD)(NO$_3$)$_2$(H$_2$O)$_5$]·3H$_2$O in case of La(III), Pr(III), Nd(III), Sm(III), Eu(III), Gd(III), Tb(III) and Dy(III), and [Ln$_2$(BMSPD)(NO$_3$)$_2$(H$_2$O)$_5$] in case of Y(III). The ligand coordinates to the inner lanthanide center through pyridine nitrogen and two enolized and deprotonated carbonyl oxygens. Ligation of a bidentate nitrate and three coordinated water molecules renders the lanthanide ion eight-coordinated. The ligand coordinates through two hydrazonic nitrogens and doubly deprotonated phenolic groups to the outer metal center
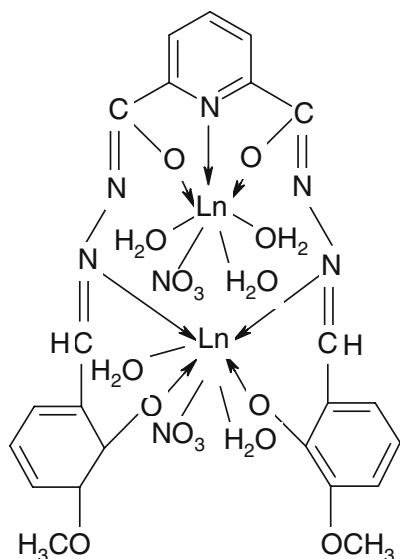
Figure 5. Proposed structure of Ln(III) complexes of BMSPD.

leading to closure of the ligand cavity. The outer lanthanide (III) ion reaches its coordination saturation through incorporation of a bidentate nitrate and two coordinated water molecules. Both the lanthanide centers are in eight-coordination environment. The homodinuclear lanthanide (III) complexes are proposed as having the tentative structure shown in Figure 5. (Note: For the sake of clarity nitrate ion has been represented with a single bond and lattice molecules have been omitted.)

From the structure, it seems that the formation of dinuclear complex is caused by the higher coordination requirements of the lanthanide ion and /or by the small cavity afforded by the heptadentate ligand. Attempts to grow crystals of these species however proved to be unsuccessful.

Acknowledgements

References

1. J.J.R.F.D. Silva and R.J.P. Williams: *The Biological Chemistry of the Elements*, Clarendron Press, Oxford (1991).
2. P.A. Brady and J.K.M. Sanders: *Chem. Soc. Rev.* **26**, 327 (1997).
3. A.J. Kirby: *Angew. Chem. Int. Ed.* **35**, 706 (1996).
4. Y. Murakami, J.-I. Kikuchi, Y. Hisaeda, and O. Hayashida: *Chem. Rev.* **96**, 721 (1996).
5. N.H. Williams, B. Takasaki, and J. Chin: *Acc. Chem. Res.* **32**, 485 (1999).
6. J. Chin: *Curr. Opin. Chem. Biol.* **1**, 514 (1997).
7. K.G. Ragunathan and H.-J. Schneider: *Angew. Chem. Int. Ed.* **35**, 1219 (1996).
8. U. Casellato, P. Guerriero, S. Tamburini, P.A. Vigato, and R.J. Graziani: *J. Chem. Soc., Dalton Trans.* 1533 (1990).
9. P. Guerriero, S. Sitran, P.A. Vigato, C. Marega, A. Marigo, and R. Zametti: *Inorg. Chim. Acta.* **171**, 103 (1990).
10. V. Balzani and R. Ballardini: *Photochem. Photobiol.* **52**, 409 (1990).
11. R.S. Davidson and M.M. Hilchenbach: *Photobiol.* **52**, 431 (1990).
12. R.F. Lauffer: *Chem. Rev.* **87**, 901 (1987).
13. J.P. Desvergne, F. Fages, H. Bouas-Laurent, and P. Marsau: *Pure Appl. Chem.* **64**, 1231 (1992).
14. L.G. Hubert-Pfalzgraf: *New J. Chem.* **19**, 727 (1995).
15. P. Chanaud, A. Julbe, P. Vaija, M. Persin, and L. Cot: *J. Mater. Sci.* **29**, 4244 (1994).
16. A. Bacchi, L.P. Battaglia, M. Carcelli, C. Pelizzi, G. Pelizzi, C. Solinas, and M.A. Zoruddu: *J. Chem. Soc. Dalton Trans.* 775 (1993).
17. G. Paolucci, S. Stelluto, and S. Sitran: *Inorg. Chim. Acta.* **110**, 19 (1985).
18. D.L. Arora, Keemti Lal, S.P. Gupta, and S.K. Sahni: *Polyhedron* **5**(10), 1499–1501 (1986).
19. B. Figgis and G. Lewis: in J. Lewis and R.J. Wilkins (eds.), The Magnetochemistry of Complex compounds in Modern Coordination Chemistry, Interscience, New York (1960).
20. F.J. Welcher: *The Analytical Use of EDTA*4, Van Nostrand, New York (1965).
21. W.J. Geary: *Coord. Chem. Rev.* **7**, 81 (1971).
22. L.J. Bellamy: *The Infra-Red Spectra of Complex Molecules*, 3rd ed.,, Chapman and Hall Ltd, London (1975).
23. M. Keeton, A.B.P. Lever, and B.S. Ramaswamy: *Can. J. Chem.* **48**, 3185 (1970).
24. V.B. Rana, S.K. Sahni, and S.K. Sangal: *J. Inorg. Nucl. Chem.* **41**, 1498–1500 (1979).
25. R.G.R. Bacon and W.S. Lindsay: *J. Chem. Soc.* 1382 (1996).
26. X.Y. Chen, S.Z. Zhan, and Q.J. Meng: *Transition Met. Chem.* **21**, 345 (1996).
27. K.K. Narang, T.R. Rao, Sabita Sreshtha, and Shankar Shreshtha: *Synth-React. Inorg. Met. – Org. Chem.* 931–954 (2000).
28. R.G. Grzeskowiak, C.W. Whatley, and M. Goldstein: *Spectrochim. Acta.* **31A**, 1577 (1975).
29. K. Nakamoto: *Infra-Red Spectra of Inorganic and Coordination Compounds*, Wiley-Interscience, New York (1970).
30. B.M. Gatehouse, S.E. Livingstone, and R.S. Nyholm: *J. Chem. Soc.* 4222 (1957).
31. N.F. Curtis and Y.M. Curtis: *Inorg. Chem.* **4**, 804 (1965).
32. Jean-Pierre Costes, Jean-Pierre Laussac, and Franck Nicodeme: *J. Chem. Soc., Dalton Trans.* 2731 (2002).
33. C. Netai Singha and D.N. Satyanarayana: *J. Mol. Struc.* **403**, 123 (1997).
34. SDBS Web: http://www.aist.go.jp/RIODB/SDBS No.2225 HSP-49–058(27–8–04).
35. SDBS Web: http://www.aist.go.jp/RIODB/SDBS No. 2329 HSP-01–166(27–8–04).
36. T. Zafiropoulos, J. Plakatouras, and S.P. Perlepes: *Polyhedron.* **10**(20/21), 2405–2415 (1991).
37. J.H. Van Vleck and A. Franck: *Phys. Rev.* 34 (1929).
38. F. Hund: *Z. Physik.* **33**, 855 (1925).
39. S.P. Sinha: *Complexes of Rare Earths*14, Pergamon Press, New York (1966).
40. T.J. Mark: *Prog. Inorg. Chem.* **24**, 57 (1978).
41. G.N. George, R.C. Prince, and R.E. Bare: *Inorg. Chem.* **35**, 434 (1996).
42. A. Siedel, H. Bill, L.P. Nordblad, and F. Kilar: V. *Arch. Biochem. Biophys.* **308**(1), 52 (1994).
43. A.J. Pierek, W.R. Hagen, W.R. Dunham, and R.H. Sands: *Eur. J. Biochem.* **206**(3), 705 (1992).
44. F.M. Ramirez, M.E. Sosa-Torres, E Basurto-Uribe, R. Zamorano Ulao, and F. Rio-Portillo: *J. Coord. Chem.* **41**, 303–326 (1997).
45. D.G. Karraker: *Inorg. Chem.* **6**, 1863 (1969).
46. C.K. Jorgenson: *Acta. Chem. Scan* **11**, 1981 (1957).
47. D.E. Henrie and G.R. Choppin: *J. Chem. Phys.* **49**, 477 (1968).
48. S.P. Sinha: *Spectrochim. Acta* **22**, 57 (1966).
49. C.K. Jorgenson: *Prog. Inorg. Chem.* **4**, 73 (1972).
50. A. Seminara, A. Musumeci, and A. Chisari: *Inorg. Chim. Acta.* **82**, 173 (1984).

51. S.P. Sinha: *Struc. Bonding.* **9**, 25 (1976).
52. J. Yoon and A.W. Czarnik: *J. Am. Chem. Soc.* **114**, 5874 (1992).
53. A. Beeby, R.S. Dickins, S. Faulkner, D. Parker, L. Royle, A.S. deSousa, J.A.G. Williams, and M. Woods: *J. Chem. Soc., Perkin Trans.* **2**, 493 (1999).
54. R.S. Dickins, T. Gunnlaugsson, D. Parker, and K.D. Peacock: *Chem. Commun.* 1643 (1998).
55. H.W. Seely and P.J. Van Demark: *Microbes in action, a laboratory manual of microbiology*, 2nd ed., R. J. Taraporewala and Co. Pvt. Ltd, Bombay, India (1970), pp. 55–80.